Ion Exchange to Capture Iron after Real Effluent Treatment by Fenton's Process

Eva Domingues [1,*], Eryk Fernandes [1], Telma Vaz [1], João Gomes [1], Sergio Castro-Silva [2], Rui C. Martins [1], Rosa Quinta-Ferreira [1] and Licínio M. Ferreira [1]

[1] CIEPQPF–Chemical Engineering Processes and Forest Products Research Center, Department of Chemical Engineering, Faculty of Sciences and Technology, University of Coimbra, Rua Sílvio Lima, 3030-790 Coimbra, Portugal; eryk@eq.uc.pt (E.F.); telma@eq.uc.pt (T.V.); jgomes@eq.uc.pt (J.G.); martins@eq.uc.pt (R.C.M); rosaqf@eq.uc.pt (R.Q.-F.); lferreira@eq.uc.pt (L.M.F.)

[2] Adventech–Advanced Environmental Technologies, Rua de Fundões 151, 3700-121 São João da Madeira, Portugal; sergio.silva@adventech-group.com

* Correspondence: evadomingues@eq.uc.pt; Tel.: +351-239-798-723; Fax: +351-239-798-703

Abstract: The main drawback of Fenton's process is the formation of ferric sludge. In this work, ion exchange (IE) appears as a complement to the Fenton process, allowing, on the one hand, to remove the iron excess present in the sludge, as well as reduce the COD of the real olive oil industry extraction wastewater (OOIEW) from the Fenton process. The Fenton process uses iron (II) sulfate as catalyst, therefore concentrations of iron up to 2 g L^{-1} could be present in the treated OOIEW. The iron and COD adsorption equilibrium behavior has been modelized by Langmuir, Freundlich and Temkin isotherms. Moreover, the resin efficiency was tested in a continuous fixed-bed column. It was concluded that the resin maintains iron adsorption capacity over at least three reuse cycles. Overall Fenton's process followed by ion exchange seems to be a promising approach for the treatment of cumbersome industrial wastewaters.

Keywords: fenton process; iron sludge; strong acid cation exchange; olive oil extraction; fenton process

1. Introduction

The future availability and quality of water has become a common agenda of different nations and institutions. As a reflection of this situation, new and optimized water treatment technology development has been the focus of the scientific community in order to overcome the water contamination problematic. Besides the need of a technology that can achieve a high efficiency of the degradation of compounds with multiple hazardous characteristics, such as toxicity and persistent behavior, the economical aspect needs to be evaluated to obtain a feasible treatment alternative that can be applied at larger scales.

The advanced oxidation processes (AOPs) are a group of interesting technologies, vastly applied in water treatment, as they are based on reactions involving species with high oxidative potentials that are highly efficient and non-selective [1]. In fact, AOPs under certain conditions can transform different organic compounds into less hazardous and complex molecules, such as H_2O, CO_2, and other inorganic ions, as products of the respective oxidation reactions [2]. The Fenton reaction is part of the AOPs group, appearing as an attractive alternative to conventional treatment methods of effluents, in particular as it contains a high concentration of recalcitrant compounds, namely olive oil production effluents [3].

Fenton's reagents applied in the reactions are hydrogen peroxide (H_2O_2) and an iron ions source, which are considerably simple and taken as a greatly effective method for organic pollutants oxidation, already applied in a variety of wastewaters [1,4]. The high efficiency of the method is a result of strong hydroxyl radicals (HO*) formation and change of oxidation state of Fe^{2+} in Fe^{3+} [5]. Both iron ions are coagulants, so Fenton's reaction

combines both oxidation and coagulation treatments [6]. The operating conditions that best suit the target effluent are required to be specifically optimized to achieve optimum degradation efficiencies. Fenton's process is dependent on pH, Fenton reagents' concentration and ratio, and initial organic pollutants concentration [7]. The possibility of being performed at room temperature and the fact that the pressure conditions use innocuous and easy to handle reactants, as well as the high elimination rates reached are the main advantages of this method [8]. However, Fenton's process also has drawbacks; namely, it is typically restricted to low pHs, contains elevated H_2O_2 doses, and the buildup of ferric sludge affects the oxidation efficiency [3,9].

Iron is the most commonly used metal catalyst, due to its abundant availability and lower price [4]. The use of a homogeneous iron catalyst in the process leads to an elevated concentration of dissolved iron in the treated liquid post oxidation. Metals may possess toxic effects to living organisms including humans when in very high concentration [10]. Thus, environmental legislation establishes strict limits for metals in discharged wastewater.

The Portuguese environmental legislation (DL 236/98) establishes a maximum limit of 2.0 mg L^{-1} of total iron, for the release of wastewater into the natural water bodies and for public water source. Therefore, Fenton's is usually followed by an additional separation method regarding its iron content, prior to the effluent's disposal [11]. Metal ions are commonly removed by chemical precipitation. However, this generates severe drawback, as it leads to a large sludge volume, requiring an additional post management and disposal [12]. Furthermore, the iron concentration in the liquid may be still high even after the precipitation step. Moreover, the catalyst recovery is not possible.

Currently, the ion exchange (IE) process is taken as a very effective method of separation dissolved compounds, due mainly to its low cost, ease of handling, small requirement of reagents, and the possible retrieval of added-value components through the formation of adsorbent/IE resin [13]. Different materials can be applied as sorbent, such as synthetic resins with different characteristics [11,14–17], synthetic and natural zeolites [18,19] and algae [20].

To surpass the disadvantage of homogeneous Fenton's reaction producing sludge, this present study focuses on the investigation of an alternative strategy for the management and treatment of the resultant real wastewater of an olive oil extraction process (OOEIW). This strategy comprises the implementation of Fenton's process for organic degradation, followed by an iron recuperation step, applying Amberlite@HPR1100 strong-acid cationic resin. The iron load influence in the pretreated olive oil extraction wastewater (POOEIW) stream was investigated for 1–2 g L^{-1} range. The equilibrium behavior of this ion has been studied by the application of different prediction models (Langmuir, Freundlich and Temkin). Other empirical models were additionally used for the description of the sorption process dynamics in a continuous fixed-bed column when different experimental conditions were considered. The suggested IE procedure suitability and characteristics of the adsorbent post regeneration was evaluated. Moreover, the possibility of IE resin removing organic matter from the wastewater was evaluated.

Some studies have been undertaken for iron recovery after the Fenton process and its reuse in the Fenton-like process [21,22]. However, to the best of our knowledge, this is the first time such an approach has been applied to a real wastewater with a very high organic load (~50 gO_2 L^{-1}). This high COD implies the use of a high load of iron which increases the complexity of IEX process. The performance of the resin in the removal of COD, as well as the interference of the organic load in the removal of the iron, was explored for the first time to the best of our knowledge. In addition, which types of pollutants are more selective to the resin among the organic matter in the real effluent was investigated. Therefore, this study builds on previous studies but accounts for relevant factors that have not been mentioned before.

2. Materials and Methods

2.1. Ion Exchange Resin and Chemicals

Amberlite@HPR1100 resin, provided by Sigma-Aldrich (St. Louis, MO, USA), physically and chemically characterized in Table 1, was used in the IE tests.

Table 1. Physical characteristics of Amberlite@HPR1100.

Appereance [a]	Amber, translucent, spherical beads
Copolymer, Matrix [a]	Styrene-divinylbenzene, Gel
Functional group [a]	Sulfonic acid
Ionic Form as Shipped [a]	Na^+
Particle diameter [a] (μm)	585 ± 5
Surface area [b] (m^2/g)	0.673
Average pore diameter [b] (nm)	2.595
Pore volume [b] (cm^3/g)	0.0004
Real density [b] (g/cm^3)	1.227

[a] Information obtained by the supplier. [b] Determined by nitrogen porosimetry.

The chemicals heptahydrate iron sulfate, hydrogen peroxide, sulphuric acid and sodium hydroxide were obtained from PanReac.

The real effluent comes from a refined oil extraction plant located in Center region of Portugal. Wet olive mills waste, resulting from the production of olive oil in two phase process, are used for oil extraction. While waiting to be processed, these wastes are stored and a dark colored and highly charged liquid leaches; also, during the waste processing and before extraction a wastewater is produced. The olive mill wastewaters formed are collected and stored in tanks because no efficient treatment approach is available. For this study, samples collected from the tank were stored in 25 L plastic containers to later be used in the laboratory.

2.2. Experimental Procedures

2.2.1. Fenton's Reaction

Fenton's tests were carried out in a batch stirred reactor (0.5 L at 700 rpm) for a homogeneous mixture. The catalyst, $FeSO_4.7H_2O$, was added to the effluent and with addition of H_2SO_4 the pH was adjusted to 3 due to iron's solubility and to ensure higher reaction rate. The solution was then mixed for 5 min to assure total homogeneity, and the addition of the required volume of 33% w/v H_2O_2 represented the start of the reaction. After reaction (60 min), the effluent goes directly to the IE process.

The conditions for the Fenton reaction were previously optimized by Domingues et al. (2021): pH 3; $[H_2O_2]$ = 4 g L^{-1}; $[Fe^{2+}]$ = 2 g L^{-1} and t = 60 min. Physicochemical characteristics of OOEIW after Fenton (FOOEIW) process, which will be used later in IE, are presented in Table 2.

Table 2. Physico-chemical characterization of OOEIW before and after Fenton's process.

Parameter	Before Fenton Process	After Fenton Process
pH	4.8 ± 0.3	3–3.4
COD (g O_2 L^{-1})	50.4 ± 5	17.5–22.5
BOD5 (mg O_2 L^{-1})	8000 ± 800	770–1100
Biodegradability (BOD_5/COD) (%)	0.16 ± 0.05	44
$[Fe^{3+}]$ (g L^{-1})	0	~2

2.2.2. Batch Adsorption Experiments

Amberlite@HPR1100 was washed with several cycles of 1.0 M HCl, 1.0 M NaOH and water for removing solvents and other impurities, in a fixed-bed column, before being used as adsorbent. The last conditioning step consisted of contacting the resin with a

HCl solution (1.5 M) to convert it to the H^+ form. The resin was regenerated, repeating the conditioned method before being referred after each operational cycle. To determine equilibrium isotherms, batch tests were performed by contacting 20 or 40 mL of iron solutions with olive oil extraction wastewater of a known concentration with different conditioned resin amounts (0.2–5.4 g) at pH 3 (characteristic pH of the Fenton reaction). The sealed flasks were continuously stirred in a thermostatic bath for 24 h at constant temperature (25 °C) until equilibrium was reached. In the end, the solid (resin) and liquid phase were separated by filtration and the amount of iron in the liquid phase, quantified. The amount of iron absorbed, q_e (mg/g), by the resin was calculated by the Equation (1):

$$q_e = (C_0 - C_e)V/m \tag{1}$$

where C_0 and C_e are the metal ion concentration in the beginning and equilibrium phase (mg L^{-1}), respectively, V is the amount of solution (L) and m is the mass of resin used (g).

In order to infer the role of adsorption in the real wastewater chemical oxygen demand (COD) abatement, some batch IE experiments were also performed with simulated effluents. Thus, a synthetic solution of humic acid (Sigma-Aldrich) with the same COD of the real effluent tested was mixed with iron sulphate (the same load applied in Fenton's process–2 g L^{-1}) and subjected to IE experiments at batch conditions. The same was performed but with a synthetic solution of 5 phenolic acids (trans-cinnamic, 3,4-dimethoxybenzoic, 4-hydroxybenzoic, 3,4,5-trimethoxybenzoic and 3,4-dihydroxybenzoic acid) at 100 mg L^{-1} each. These acids are known to be part of the composition of the real wastewater.

Freundlich, Langmuir, Temkin and Langmuir–Freundlich isotherm models described the equilibrium characteristics of sorption of Fe^{2+} ions by the resin Equations (2)–(5), respectively:

$$q_e = q_{max}K_LC_e \ /(1 + K_LC_e) \tag{2}$$

$$q_e = K_FC_e^{nF} \tag{3}$$

$$q_e = Bln(AC_e) \tag{4}$$

$$q_e = Q_m(K_aC_e)^n/1 + (K_aC_e)^n \tag{5}$$

The maximum absorption capacity by the absorbent is q_{max} (mg g^{-1}) the Langmuir constant correlated to the energy of adsorption is K_L (L mg^{-1}) [23,24]; the Freundlich constant is K_F ($mg^{1-(1/n)}L^{1/n}$ g^{-1}) and the heterogeneity of the adsorbent surface is described by n_F, the equilibrium constant suggestive of adsorption intensity [25]. The Temkin model takes into consideration the effect of interactions on the adsorption process between adsorbent (resin) and adsorbate (iron) [26]. The parameter A (L mg^{-1}) is the equilibrium binding constant, and B (J mol^{-1}) is the Temkin constant associated to the heat of adsorption.

The Langmuir–Freundlich isotherm considers both the Langmuir-type and Freundlich-type adsorption. The adsorption capacity of the technique is represented by Q_m (mg of sorbate/g sorbant), the concentration in aqueous phase at equilibrium is C_{eq} (mg L^{-1}), the affinity constant for adsorption is defined by K_a is (L mg^{-1}) and the level of heterogeneity is represented by n. The Langmuir–Freundlich isotherm permits classifying the density function for heterogeneous systems using a heterogeneity index n, which is allowed to vary from 0 to 1. For a homogeneous material the value of n is 1, and for heterogeneous materials it is less than one [27,28].

The Fe^{3+} removal efficiency, R, was calculated by Equation (8), as a function of resin dosage (m/V). This equation results by combining the solute mass balance in Equation (6), the efficiency definition in Equation (7), and Langmuir equilibrium isotherm in Equation (2):

$$VC_0 = VC_e + mq_e \tag{6}$$

$$R = (C_0 - C_e)/C_0 \tag{7}$$

$$C_0 - C_0(1 - R) - \left[\frac{q_{max}K_LC_0(1 - R)}{1 + K_LC_0(1 - R)}\right]\frac{m}{V} = 0 \qquad (8)$$

2.2.3. Ion Exchange Continuous Experiments

For IE experiments, a continuous packed bed column system was used, containing Amberlite@HPR1100, and a peristaltic pump (Minioplus3-Gilson) to move the treated effluent. The IE column was made of a glass tube (120 mm height × 15 mm internal diameter).

During the whole experiment, the feed solution was continuously stirred. The flow rate was also a parameter studied (5–15 mL min^{-1}) as well as the amount of resin. The initial pH of feed solution was ~3 (the optimal pH for Fenton's process).

Different initial concentration of iron was examined in terms of absorption capacity, at the levels: 1–2 g L^{-1}.

At the exit of the column, samples were collected for iron and chemical oxygen demand (COD) analysis. The fraction of the saturated bed (*FSB*), is defined by Equation (9) and quantifies the ratio between the total mass of Fe^{3+} adsorbed in the column until the breakthrough time, t_{bp}, and the mass of iron introduced into the column until equilibrium:

$$FSB = \frac{\int_0^{tbp}\left(1 - \frac{C}{Ce}\right)dt}{\int_0^{\infty}(1 - \frac{C}{Ce})dt} \qquad (9)$$

the time required to the exit concentration, *C*, is denominated by t_{bp} and is about 1% of C_e; t_{ex} is about 95% of C_e and is the time required to C, t_{st} can be expressed by Equation (10):

$$t_{st} = \int_0^{\infty}(1 - \frac{C}{Ce})dt \qquad (10)$$

2.3. Analytical Techniques

The chemical oxygen demand (COD) was assessed according to the standard method [29], where the sample was digested in an ECO 25 thermoreactor during 2 h at 150 °C. After cooling the mixture, using a Photolab S& WTW, the absorbance was measured at 605 nm. For the calibration curve, a solution of potassium hydrogen was used.

For pH determination an automatic pH meter (Crison micropH 2002) was used.

For iron quantification in the liquid phase a flame atomic absorption spectrophotometry (Perkin Elmer 3300) was used.

For the analysis of the synthetic solution of phenolic acids in the HPLC, the used method was according to Domingues et al. [30] at 40 °C, with a C18 column (SiliaChrom). The mobile phase with a 50/50 mixture of methanol and acidified water, with 1% orthophosphoric acid, had a flow rate of 0.5 mL min^{-1} and. At 255 nm, the peak determination and phenolic acids identification were determined.

3. Results and Discussion

3.1. Adsorption Equilibrium Isotherms

The main objective of the use of ion-exchange technology is to withdraw the iron from the sludge resulting from the Fenton process. The Fenton reaction occurs at pH~3, thus, industrially it is longer necessary to alkalinize the effluent after Fenton's process to promote iron precipitation. The goal is to directly send the Fenton's treated effluent to the IE process. According to Víctor-Ortega et al. [22], during the IE process the removal efficiency of iron ions increases with an increase in the initial pH up to a value equal to 4. At moderate pH with an initial pH on the range of 3–5 the linked H$^+$ is free from the active sites of the cation exchange resin, which favors the exchange of ions, thus considering the acidic environment beneficial. On the other hand, by increasing the initial pH, there will be lower IE removal efficiencies due to the precipitation of metallic hydroxides as the dominant mechanism and, consequently, lower cation exchange capacity. The pH effect was a parameter widely

studied by other authors [31,32], who corroborated the benefit of a low pH in equilibrium isotherms. For a correct assessment in terms of COD and dissolved iron removal, in this work the Fenton reaction was stopped, using a NaOH solution to increase the pH to 11. Before IE the pH was again adjusted to 3, thus re-dissolving the iron.

The outcome of adsorbent dosage on Fe^{3+} and COD removal was evaluated, changing the initial concentration of iron and COD. The results are presented in Figure 1.
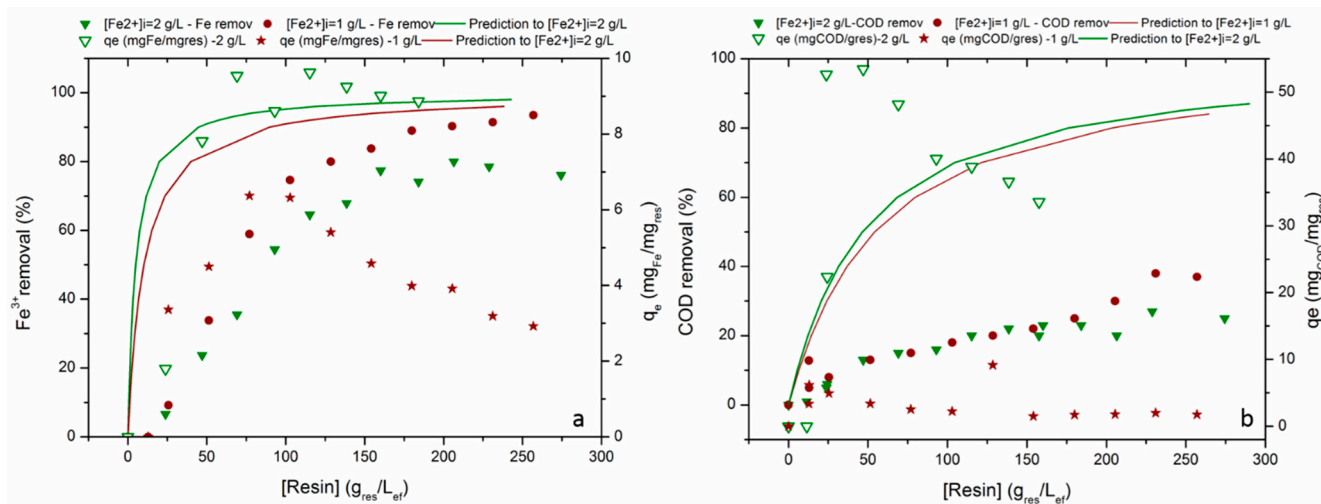

Figure 1. (**a**) Effect of adsorbent dosage on Fe^{3+} and (**b**) COD removal by Amberlite HP1100 in OOIEW pretreated by Fenton's process.

Figure 1 shows that the increase on the adsorbent load up to the approximate value of 175 g_{res}/L_{ef} improves both iron and COD removal. From this value onwards, removals are constant in the order of 90 and 80% for iron and 20 and 30% for COD, considering an initial concentration of 1 and 2 g L^{-1} of iron, respectively. These results are extremely interesting, as the effluent presents a high organic load; with IE it is possible, on the one hand, to face the great disadvantage of the Fenton's process, which is the formation of iron sludge, allowing the iron limits required in the discharge of the effluent to be met. On the other hand, the effluents COD can be further removed after the Fenton process.

From Figure 1a it is still possible to evaluate the effect of iron initial concentration on IE removal efficiency. Iron concentration was evaluated between 1–2 g L^{-1} and the results showed that the adsorption of ions by the resin was strongly affected by its initial concentration. When the feed has a lower iron concentration, for the same resin load, higher iron removal is achieved. This decrease in iron removal with increasing iron initial concentration is related to IE resin saturation [16,33]. Bulai and Cionca [34] reported a loss in the iron removal effectiveness with Purolite S930-H resin from 95%, with an initial concentration of 10 mg L^{-1} to 20% for an initial concentration of 300 mg L^{-1} considering a resin concentration equal to 1.0 g L^{-1}.

The prediction models are based on Equation (8) and Langmuir model parameters, considering the initial concentrations of Iron (1 and 2 g L^{-1}) and the initial concentrations of COD (23 and 20 g L^{-1}). The prediction for iron removal is closer to experimental values than the one presented for COD removal. The effluent heterogeneity certainly contributes to having an optimistic model in relation to the experimental values.

The classic Langmuir [35], Freundlich, Temkin and Langmuir–Freundlich models were selected to describe the equilibrium experimental data for Amberlite@HPR1100 resin regarding iron and COD removal from real OOIEW after Fenton's process (Figure 2).
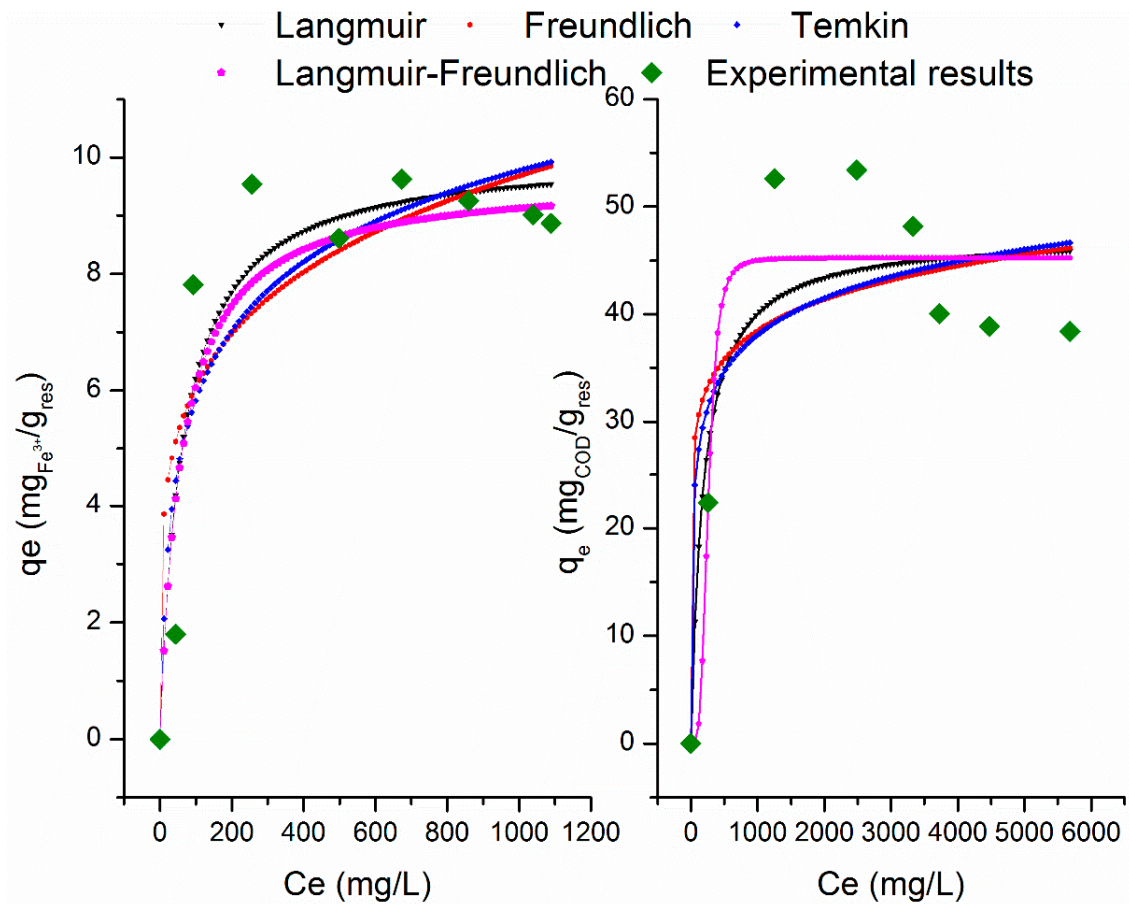
Figure 2. Adsorption isotherms of COD on Amberlite@HPR1100, and fitting through Langmuir, Freundlich and Temkin models for a feed concentration of 2 g L^{-1} of iron.

Three equilibrium models, Langmuir, Freundlich and Temkin, were used for the experimental data analysis. The parameters of these isotherms were predictable by the nonlinear regression method and are summarized in Table 3.

Table 3. Parameters values of equilibrium models.

	Langmuir			Freundlich			Temkin			Langmuir–Freundlich			
	K_L (L m g^{-1})	q_{max} (mg g^{-1})	R^2	K_F (mg$^{1-(1/n)}$ L$^{1/n}$/g)	n_F	R^2	A (L g^{-1})	B (J mol^{-1})	R^2	Qm (mg g^{-1})	Ka (L m g^{-1})	n	R^2
Fe^{3+}	0.02	10.09	0.87	2.37	0.20	0.77	0.30	1.71	0.81	9.66	0.02	1	0.84
COD	0.01	47.35	0.80	18.65	0.10	0.71	2.29	4.92	0.72	—	–		—

The equilibrium data for Fe^{3+} sorption onto Amberlite@HPR1100 can be well described by Langmuir and Langmuir–Freundlich isotherms considering the values of coefficients of determination (R^2), shown in Table 3. The values of R^2 are around 0.80, not as high as they usually appear in the literature for synthetic mixtures, but one must safeguard that it is a real effluent. Thus, a strong interaction and competition between the several compounds present in this cumbersome mixture will occur. This means that several compounds can compete for the active sites in the resin. From the analysis of Table 3, it is also possible to observe that the maximum IE capacity (q_{max}) by Amberlite@HPR1100 for iron removal is 10.09 mg g^{-1}. This value is higher compared for iron adsorption onto olive stones (2.12 mg g^{-1}) [36]. On the other hand, Víctor-Ortega [16] studied iron adsorption onto

Dowex Marathon C, a strong-acid cation exchange resin, for olive mill effluent reclamation and, in this case the q_{max} was 23.27 mg g^{-1}, although the initial concentration of iron was in the range of 0.5–100 mg L^{-1} quite inferior to the 2 g L^{-1} in this study. With Purolite S930, having an initial iron concentration of 100 mg L^{-1}, the maximum experimental iron adsorption was near to 30 mg g^{-1} [34].

Another parameter that is a relevant to understanding the Langmuir isotherm is the factor separation R_L, which can be calculated by Equation (11):

$$R_{L=\frac{1}{1+K_L.C}}$$
(11)

R_L in this case is about 0.67 for an initial iron concentration of 2 g L^{-1}, which indicates favorable adsorption, and it can be observed that data fit the Langmuir isotherm model.

Regarding the Freundlich model, the value of R^2 (0.77) was found to be lower than the value of R^2 (0.87) of Langmuir isotherm. With regards the *n* coefficient, the value is higher than 1, which proves the favorability of the adsorption process. Considering Figure 2, it can be noted that Freundlich model is able to describe the adsorption experimental data with less consistency. Pehlivan and Altun [37] verified that Langmuir model fits better than the Freunlich model for the experimental data for adsorption of Cu^{2+}, Zn^{2+}, Ni^{2+}, Cd^{2+} and Pb^{2+} ions on Dowex 50 W, a strong-acid cation exchange resin. In addition, Víctor-Ortega [16] reached the same conclusion for iron removal with Dowex Marathon. C. Martins et al. [11] concluded the same when recovering iron from a treated synthetic winery effluent with Fenton's process using Lewatite TP207.

The R^2 value for the Temkin model (0.81) is inferior to that calculated for the Langmuir model (0.87) but higher than that for the Freundlich model (0.77). The parameters of the Temkin model, *A* and *B*, were presented in Table 3 and the heat of sorption process, assessed by Temkin isotherm model, is 4.80 J mol^{-1}.

Regarding COD, the Langmuir model is the one that presents the best fit with an R^2 of 0.80. The Freundlich and Temkin models have a lower fit in the order of 0.70. There is no information in the literature regarding the adjustments of the models in terms of COD; however, since it is a real and complicated effluent, one can consider the adjustments quite acceptable.

As was referred to before, it was interesting to discover that IE also allows COD removal. In order to understand the nature of the organic matter that is adsorbed by the resin, two synthetic solutions were prepared and applied in IE. In a first step, a solution of humic acid was prepared to simulate the organic matter present in the actual treated effluent (thus with the same COD) and subsequently subjected to the IE process. It was found at those conditions, and no COD removal was possible, since no COD variation was detected after the IE process. Since it is known that OOEIW has phenolic acids in its composition, the synthetic solution prepared with five was subjected to the IE process. It was verified that the resin can retain a percentage of these acids (Figure 3). To better understand which acids have a higher affinity to the resin, the samples were analyzed over time by HPLC. The results are shown in Figure 3.

By analyzing Figure 3, one can observe that the resin can remove whichever acid, with a slightly lower affinity towards trans cinnamic acid. Thus, the COD abatement observed during IE of the real POOEIW can be partially explained by the retention of some phenolic compounds in the resin.
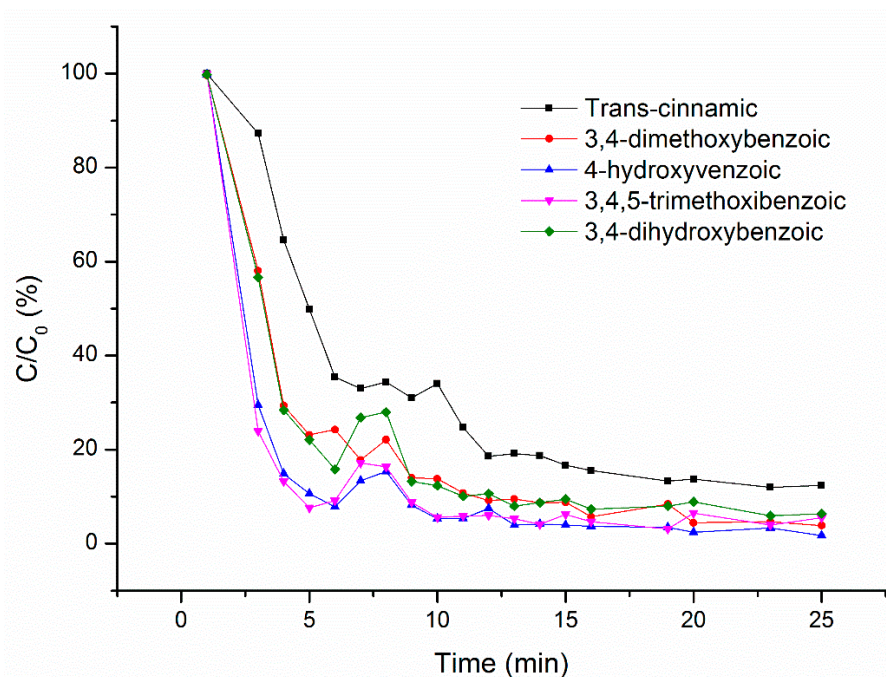
Figure 3. Phenolic acids removal by resin Amberlite@HPR1100 in a continuous packed bed column system at pH 3.

3.2. Analysis of Fe^{3+} Sorption in Continuous Process

The design of a fixed-bed sorption system considers several operational variables. In this study, the superficial velocity effect of the fluid, u_0, of mass of resin, m, and of iron initial concentration, C_e, on the IE performance was investigated. The experimental breakthrough curves and key parameters were calculated and are shown in Table 4. The results obtained were useful to identifying the optimal conditions for the liquid flowrate, Q, and mass, m, which leads to an effective column utilization.

Table 4. Experimental conditions parameters to evaluate the process performance.

Run	Q (mL min^{-1})	m (g)	q (mg g^{-1})	τ (min)	t_{st} (min)	*FSB*
1	10 (iron solut.)	8.0	9.84	0.39	5.68	0.015
2	5	8.0	9.80	0.78	13.25	0.026
3	10	8.0	9.80	0.26	4.49	0.021
4	15	8.0	9.86	0.39	5.30	0.021
5	10	13.0	9.77	0.78	14.34	0.065
6	10	18.0	9.86	1.18	16.17	0.044
7	10	55.0	9.78	3.76	68.04	0.040
8	10	36.0	9.78	2.43	43.69	0.076

The superficial velocity effect on the iron adsorption by Amberlite@HPR1100 was studied, varying the flowrate to 5, 10 and 15 mL min^{-1} and keeping the inlet iron concentration (C_0 ~2 g L^{-1}) constant at pH 3 and the mass of resin (or bed depth) at 8.0 g. Figure 4a,b show the breakthrough curves for different liquid flowrates (keeping the mass of resin constant) and different resin amounts (keeping the liquid flowrate constant), respectively. Figure 4c compares the results obtained when using the real wastewater after Fenton's process (iron C_0 ~2 g L^{-1}) with those obtained when a synthetic solution (ultrapure water containing the same concentration of iron) was applied. In both cases, a flow rate of 10 mL min^{-1} and a resin mass of 8 g were employed. Moreover, both real and synthetic wastewater were used at pH 3. The velocity variation does not affect *FSB*, while the height of fixed-bed growths this parameter. This means that with longer columns better performance is achieved.
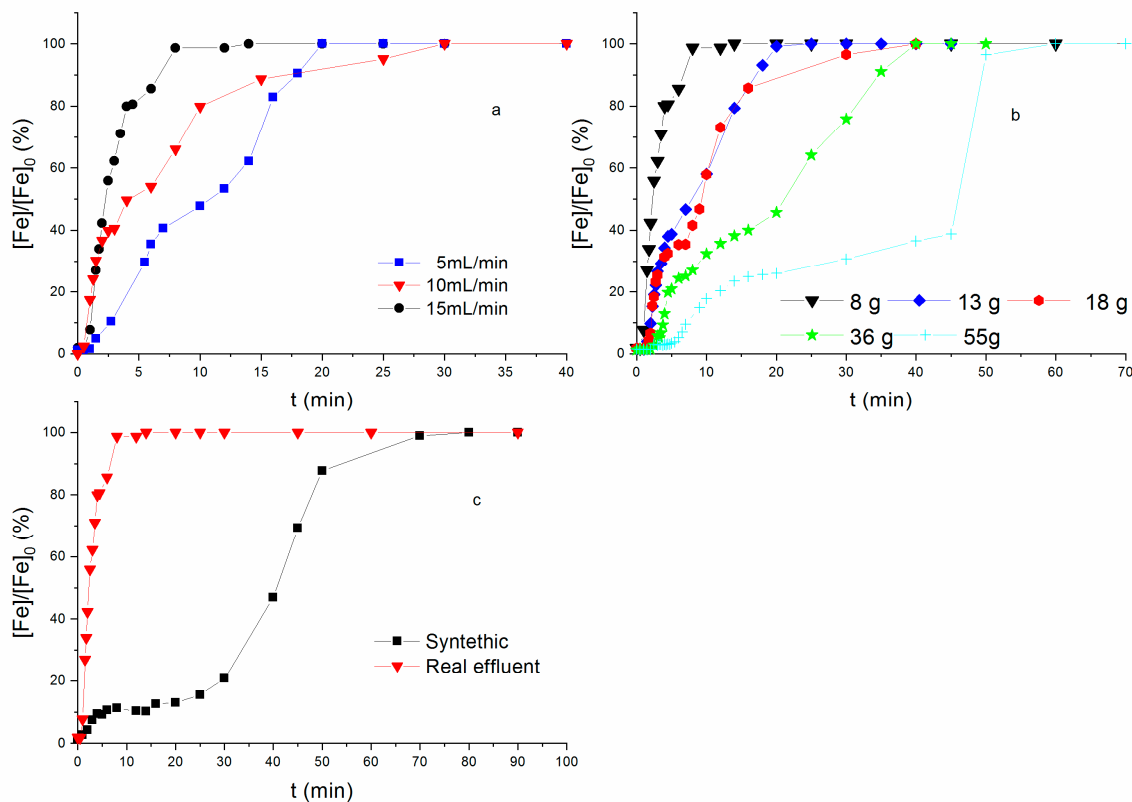
Figure 4. Breakthrough curves obtained under diverse operating settings: (**a**) Effect of the flow rate for a fixed resin mass of 8 g and feed concentration of 2 g L^{-1} of iron after a Fenton reaction with real effluent; (**b**) Effect of the resin amount for a fixed flow of 10 mL min^{-1} and feed concentration of 2 g L^{-1} of iron after a Fenton reaction with real effluent; (**c**) Comparison of IE using synthetic and real effluent after Fenton reaction with a flow rate of 10 mL min^{-1}, 8 g of resin and a feed concentration of 2 g L^{-1} of iron.

The results specified in Figure 4 and Table 4 show that, by increasing the flow rate keeping constant resin mass, the times τ and t_{st} tend to become lower for all experiments. This is justified by the fact that higher flow rate decreases the contact time between the metal ions and the adsorbent; consequentially, the mass transfer of Fe^{3+} from the solution to the adsorbent decreases.

Figure 4c shows that the resin saturates much faster when the real wastewater is applied when compared with the synthetic solution only containing iron. These results reveal that the quantity of organic matter present in the stream strongly affects the IE performance. In fact, as it was concluded from the batch experiments, this resin can remove some of the effluent COD. Most likely, phenolic acids present in its composition can adsorb in the resin surface. Thus, there will be competition between organic matter and iron ions for the solid active sites. This way, the resin will saturate faster when a complex effluent is applied when compared with cases where a synthetic solution only containing iron is used. This shows the need of testing real wastewater to design this process since the results obtained when simulated streams are applied are not transposable to real water treatment conditions.

Simplified models, namely Yoon and Nelson, Thomas and Bohard-Adams, were fitted to the experimental breakthrough curves allowing to estimate kinetic parameter related to the uptake of Fe^{3+} ions by the tested resin during its saturation in a fixed-bed. This study can be useful for the proper design, operation and reliable scale-up of the IE process. The root mean square error (*RMSE*) and the coefficient of determination (R^2) were determined and are presented in Table 5, and the fit is shown in Figure 5. These parameters allow for validating the fit of the applied models.

Table 5. Model variables for iron adsorption onto Amberlite@HPR1100.

Model	Parameter	Run							
		1	**2**	**3**	**4**	**5**	**6**	**7**	**8**
Bohard-Adams	k_{ba} (L mg^{-1} min)	0.052	0.126	0.508	0.169	0.142	0.147	0.041	0.065
	q_{ba} (mg g^{-1})	22.85	5.24	0.46	2.11	3.79	4.15	22.82	10.94
	R^2	0.97	0.98	0.98	0.93	0.97	0.96	0.90	0.96
	RMSE	1.78	0.06	0.05	0.10	0.09	0.09	1.72	0.10
Thomas	k_{th} (mL min^{-1} mg)	0.05	0.13	0.51	0.17	0.14	0.15	0.04	0.07
	q_{th} (mg g^{-1})	47.93	12.77	3.18	5.80	9.66	10.60	47.31	23.64
	R^2	0.97	0.98	0.98	0.93	0.97	0.96	0.90	0.96
	RMSE	1.78	0.06	0.05	0.10	0.09	0.09	1.72	0.10
Yoon and Nelson	k_{yn} (min^{-1})	0.10	0.25	1.02	0.34	0.28	0.29	0.08	0.13
	τ_h (min)	38.35	10.22	2.55	4.64	7.72	8.48	37.85	18.91
	R^2	0.97	0.98	0.98	0.93	0.97	0.96	0.90	0.96
	RMSE	1.78	0.06	0.05	0.10	0.09	0.09	1.72	0.10
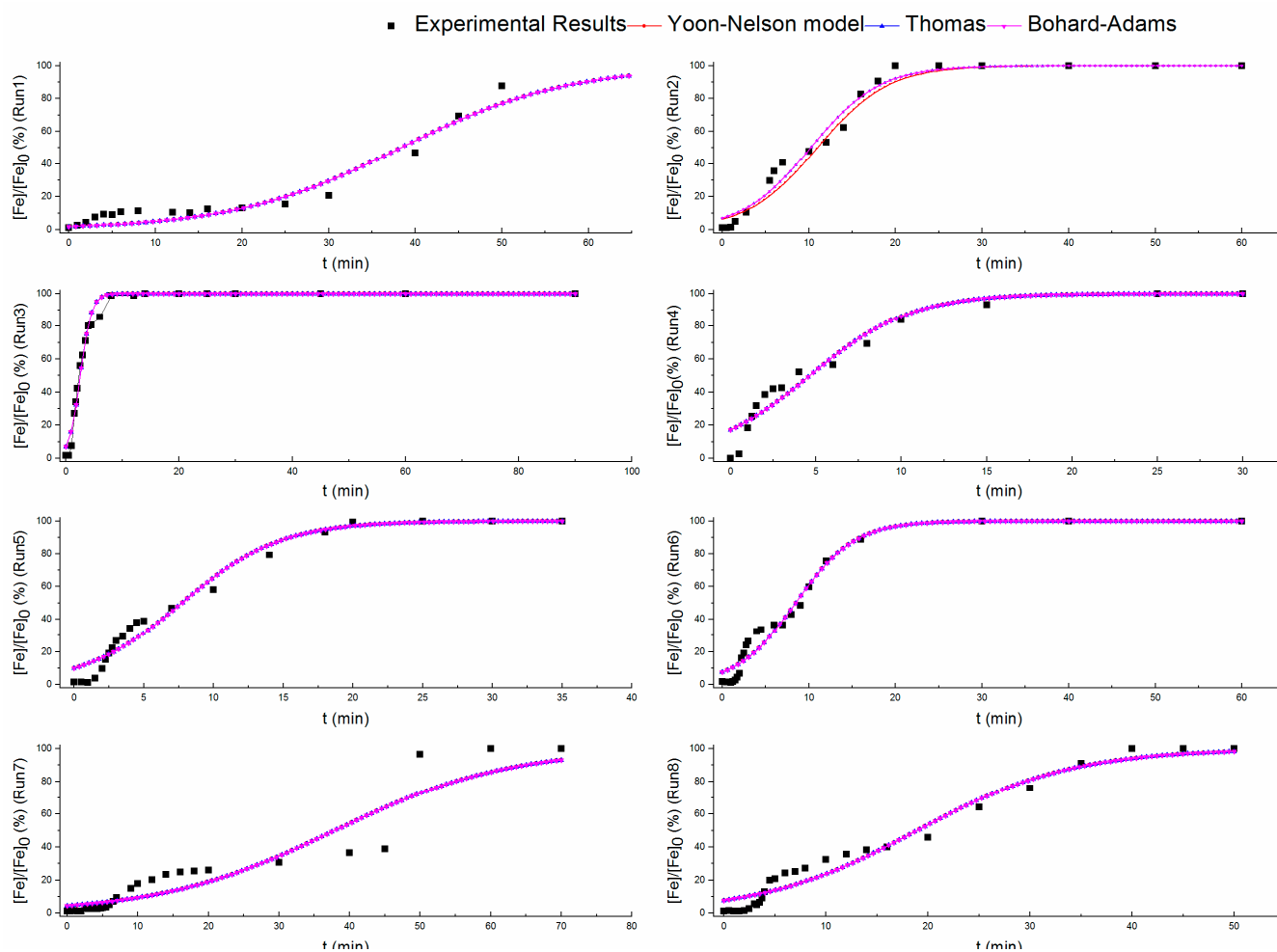
Figure 5. Saturation curves predicted by the Yoon-Nelson, Thomas and Bohard-Adams models for all experiments.

The error values obtained for the three empirical models (R^2 = 0.93–0.98 and *RMSE* = 1.72–6.25) are acceptable and there are no significant variations between them for operating conditions studied. Figure 5 represents the saturation curves predicted by the models and, as the values indicate, quite satisfactory adjustments can be observed.

3.3. Amberlite@HPR1100 Regeneration

From a financial, operational and ecological point of view, the study of resin reuse is extremely important. Figure 6 presents results in terms of iron and COD removal efficiency from resin reuse.
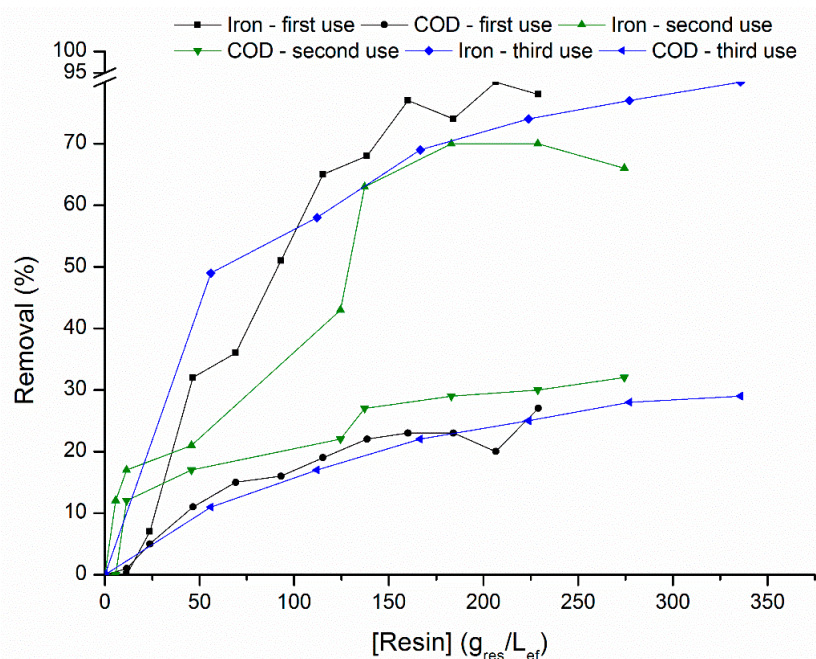

Figure 6. Amberlite@HPR1100 resin reuse (Adsorption: 2 g Fe L^{-1}, real effluent OOIEW).

The regeneration process—adsorption-desorption-washing—was supported for three cycles in the batch, as described in Section 2.2.2, using several resin loads. It was observed that after three cycles, at 215 g$_{res}$/L$_{ef}$, the iron removal capacity of the resin decreased from ~80% to 68%. Iron desorption should be close to 100% according to proposal protocol. In an acidic medium, protons compete with iron ions and can release the adsorbed iron almost completely. Consequently, some authors have also resorted to hydrochloric acid solutions to remove iron from strong acid cation exchange resins, similar to those used in this study. Millar et al. [31] achieved iron regeneration with efficiencies greater than 90% using 10% HCl and with 5% HCL: regeneration efficiencies of 89.6%. After 10 cycles of reuse, Víctor-Ortega et al. [22] reported that 100% recovery efficiencies were maintained.

The presence of organic matter in the real wastewater challenges iron adsorption since there is competition between iron ions and organic matter for the active sites. In addition, organic matter will likely challenge the resin regeneration. The desorption of these compounds can be more difficult and thus compromise the complete resin regeneration. Interestingly, COD removal was not very much affected by the regeneration process. Indeed, the third reuse of the resin leads to COD removals very similar to those obtained for the first use.

4. Conclusions

This study investigated the effectiveness of a fixed-bed IE process with a strong-acid cation exchange resin for the final iron sludge free Fenton process to treat an olive oil extraction industry wastewater.

Adsorption isotherms were studied, and analytical isotherm equations such as Langmuir, Freundlich and Temkin isotherms, which are extensively used for modeling adsorption data, were fitting with acceptable values considering the complex real effluent.

Breakthrough curves proved up to 75% maximum iron adsorption capacity onto Amberlite@HPR1100 resin, for a feed concentration of 2 g_{Fe3+} L^{-1}, and an efficiency for COD removal of 30% for an initial COD between 17.5–22.5 gO_2 L^{-1}.

The experimental breakthrough curves were well adjusted by the Bohard-Adams, Thomas and Yoon–Nelson empirical models.

Resin reuse proved to be viable, as it maintains its capacity over the cycles. With these features, the IE process could permit iron reuse in the Fenton reactor as a catalyst, which would balance the cost-effectiveness ratio of the integral process, minimizing or even avoiding the need for acid and iron to foment the Fenton reaction.

Conflicts of Interest: The authors declare no conflict of interest.

References

1. Lucas, M.S.; Dias, A.A.; Sampaio, A.; Amaral, C.; Peres, J.A. Degradation of a textile reactive Azo dye by a combined chemical-biological process: Fenton's reagent-yeast. *Water Res.* **2007**, *41*, 1103–1109. [CrossRef]
2. Gallard, H.; De Laat, J. Kinetic modeling of Fe(III)/H$_2$O$_2$ oxidation reactions in dilute aqueous solution using atrazine as a model organic compounds. *Water Res.* **2000**, *34*, 3107–3116. [CrossRef]
3. Domingues, E.; Gomes, J.; Quina, M.J.; Quinta-Ferreira, R.M.; Martins, R.C. Detoxification of Olive Mill Wastewaters by Fenton's Process. *Catalysts* **2018**, *8*, 662. [CrossRef]
4. Hussain, S.; Aneggi, E.; Goi, D. Catalytic activity of metals in heterogeneous Fenton-like oxidation of wastewater contaminants: A review. *Environ. Chem. Lett.* **2021**, *19*, 2405–2424. [CrossRef]
5. Santos, M.S.F.; Alves, A.; Madeira, L.M. Paraquat removal from water by oxidation with Fento's reagent. *Chem. Eng. J.* **2011**, *175*, 279–290. [CrossRef]
6. Badawy, M.I.; Ali, M.E.M. Fenton's peroxidation and coagulation processes for the treatment of combined industrial and domestic wastewater. *J. Hazard. Mater.* **2006**, *136*, 961–966. [CrossRef]
7. Domingues, E.; Fernandes, E.; Gomes, J.; Castro-Silva, S.; Martins, R.C. Olive oil extraction industry wastewater treatment by coagulation and Fenton's process. *J. Water Process. Eng.* **2021**, *39*, 101818. [CrossRef]
8. Duarte, F.; Maldonado-Hódar, F.J.; Madeira, L.M. Influence of the characteristics of carbon materials on their behavior as heterogeneous Fenton catalysts for the elimination of the azo dye Orange II from aqueous solutions. *Appl. Catal. B Environ.* **2011**, *103*, 109–115. [CrossRef]
9. Wang, N.N.; Zheng, T.; Zhang, G.S.; Wang, P. A review on Fenton-like processes for organic wastewater treatment. *J. Environ. Chem. Eng.* **2016**, *4*, 762–787. [CrossRef]
10. Volesky, B. Detoxification of metal-bearing effluents: Biosorption for the nextcentury. *Hydrometallurgy* **2001**, *59*, 203–216. [CrossRef]
11. Martins, P.J.M.; Reis, P.M.; Martins, R.C.; Gando-Ferreira, L.M.; Quinta-Ferreira, R.M. Iron recovery from the Fenton's treatment of winery effluent using an ion-exchange resin. *J. Mol. Liq.* **2017**, *242*, 505–511. [CrossRef]
12. Ostroski, I.C.; Barros, M.A.S.D.; Silva, E.A.; Dantas, J.H.; Arroyo, P.A.; Lima, O.C.M. A comparative study for the ion exchange of Fe(III) and Zn(II) on zeolite NaY. *J. Hazard. Mater.* **2009**, *161*, 1404–1412. [CrossRef] [PubMed]
13. Abdel-Ghani, N.T.; Hefny, M.; El-Chagbaby, G.A.F. Removal of lead from aqueous solution using low cost abundantly available adsorbents. *Int. J. Environ. Sci. Technol.* **2007**, *4*, 67–73. [CrossRef]
14. Marañón, E.; Suárez, F.; Alonso, F.; Fernández, Y.; Sastre, H. Preliminary study of iron removal from hydrochloric pickling liquor by ion exchange. *Ind. Eng. Chem. Res.* **1999**, *38*, 2782–2786. [CrossRef]
15. Üstün, G.E.; Solmaz, S.K.A.; Birgül, A. Regeneration of industrial district wastewater using a combination of Fenton process and ion exchange—A case study. *Resour. Conserv. Recycl.* **2007**, *52*, 425–440. [CrossRef]

16. Víctor-Ortega, J.M.; Ochando-Pulido, A.; Martínez-Ferez, A. Thermodynamic and kinetic studies on iron removal by means of a novel strong-acid cation exchange resin for olive mill effluent reclamation. *Ecol. Eng.* **2016**, *86*, 53–59. [CrossRef]

17. Silva, L.G.M.; Moreira, F.C.; Cechinel, M.A.P.; Mazur, L.-P.; Ulson de Souza, A.A.; Souza, S.M.A.G.U.; Boaventura, R.A.R.; Vilar, V.J.P. Integration of Fenton's reaction-based processes and cation exchange processes in textile wastewater treatment as a strategy for water reuse. *J. Environ. Manag.* **2020**, *272*, 111082. [CrossRef]

18. Al-Anber, M.; Al-Anber, Z.A. Utilization of natural zeolite as ion-exchange and sorbent material in the removal of iron. *Desalination* **2008**, *225*, 70–81. [CrossRef]

19. Kim, J.S.; Zhang, L.; Keane, M.A. Removal of iron from aqueous solutions by ion exchange with a Na-Y zeolite. *Sep. Sci. Technol.* **2001**, *36*, 1509–1525. [CrossRef]

20. Mane, P.C.; Bhosle, A.B. Bioremoval of some metals by living algae *Spirogyra* sp. *and Spirullina sp. from aqueous solution. Int. J. Environ. Res.* **2012**, *6*, 571–576.

21. García-Rodríguez, O.; Bañuelos, J.A.; Godínez, L.A.; Valdez, H.C.A.; Zamudio, E.; Ramírez, V.; Rodríguez-Valdez, F.J. Iron Supported on Ion Exchange Resin as Source of Iron for Fenton Reagent: A Heterogeneous or a Homogeneous Fenton Reagent Generation? *Int. J. Chem. React.* **2017**, *15*, 20170026. [CrossRef]

22. Víctor-Ortega, J.M.; Ochando-Pulido, A.; Martínez-Ferez, A. Iron removal and reuse from Fenton-like pretreated olive mill wastewater with novel strong-acid cation exchange resin fixed-bed column. *J. Ind. Eng. Chem.* **2016**, *36*, 298–305. [CrossRef]

23. Gupta, V.K. Application of low-cost adsorbents for dye removal—A review. *J. Environ. Manag.* **2009**, *90*, 2313–2342. [CrossRef] [PubMed]

24. Abbas, S.H.; Ismail, I.M.; Mostafa, T.M.; Sulaymon, A.H. Biosorption of Heavy Metals: A Review. *J. Chem. Sci. Technol.* **2014**, *3*, 74–102.

25. Freundlich, H. Over the adsorption in solution. *J. Phys Chem.* **1906**, *57*, 385–470.

26. Temkin, M.J.; Pyzhev, V. Recent modifications to Langmuir isotherms. *Acta Phys.-Chim. Sin.* **1940**, *12*, 217–222.

27. Turiel, E.; Perez-Conde, C.; Martin-Esteban, A. Assessment of the cross-reactivity and binding sites characterisation of a propazine-imprinted polymer using the Langmuir-Freundlich isotherm. *Analyst* **2003**, *128*, 137–141. [CrossRef]

28. Umpleby, R.J.; Baxter, S.C.; Chen, Y.; Shah, R.N.; Shimizu, K.D. Characterization of Molecularly Imprinted Polymers with the Langmuir- Freundlich Isotherm. *Anal. Chem.* **2001**, *73*, 4584–4591. [CrossRef]

29. Greenberg, A.; Clesceri, I.; Eaton, A. *Standard Methods for the Examination of Water and Wastewater*, 16th ed.; American Public Health Association (APHA): Washington, DC, USA, 1985.

30. Domingues, E.; Assunção, N.; Gomes, J.; Lopes, D.V.; Frade, J.R.; Quina, M.J.; Quinta-Ferreira, R.M.; Martins, R.C. Catalytic Efficiency of Red Mud for the Degradation of Olive Mill Wastewater through Heterogeneous Fenton's Process. *Water* **2019**, *11*, 1183. [CrossRef]

31. Millar, G.J.; Schot, A.; Couperthwaite, S.J.; Shilling, A.; Nuttall, K.; Bruyn, M. Equilibrium and column studies of iron exchange with strong acid cation resin. *J. Environ. Chem. Eng.* **2015**, *3*, 373–385. [CrossRef]

32. Rao, K.S.; Dash, P.K.; Sarangi, D.; Chaudhury, G.R.; Misra, V.N. Treatment of wastewater containing Pb and Fe using ion-exchange techniques. *J. Chem. Technol. Biotechnol.* **2005**, *80*, 892.

33. Senthil Kumar, P.; Gayathri, R. Adsorption of Pb^{2+} ions from aqueous solutions onto bael tree leaf powder: Isotherms, kinetics and thermodynamics study. *J. Eng. Sci. Technol.* **2009**, *4*, 381–399.

34. Bulai, P.; Cioanca, E. Iron removal from wastewater using chelating resin Purolite S930. *TEHNOMUS J.* **2011**, *18*, 64–67.

35. Langmuir, I. The adsorption of gases on plane surfaces of glass, mica and platinum. *J. Am. Chem. Soc.* **1918**, *40*, 1361–1403. [CrossRef]

36. Hodaifa, G.; Ochando-Pulido, J.M.; Alami, S.B.D.; Rodríguez-Vives, S.; Martínez-Férez, A. Kinetic and thermodynamic parameters of iron adsorption onto olivestones. *Ind. Crop. Prod.* **2013**, *49*, 526–534. [CrossRef]

37. Pehlivan, E.; Altun, T. The study of various parameters affecting the ion exchange of Cu^{2+}, Zn^{2+}, Ni^{2+}, Cd^{2+}, and Pb^{2+} from aqueous solution on Dowex 50W synthetic resin. *J. Hazard. Mater.* **2006**, *134*, 149–156. [CrossRef]